

# Photochemical transformation of azoxystrobin in aqueous solutions

A. Boudina<sup>a,b</sup>, C. Emmelin<sup>a</sup>, A. Baaliouamer<sup>b</sup>, O. Païssé<sup>c</sup>, J.M. Chovelon<sup>a,\*</sup>

<sup>a</sup> *Institut de Recherches sur la Catalyse et l'Environnement, (IRCELYON) UMR CNRS 5256, Université de Lyon I. 43, Boulevard du 11 novembre 1918, 69622 Villeurbanne Cedex, France*

<sup>b</sup> *Laboratoire d'Analyse Organique Fonctionnelle, Institut de Chimie, U.S.T.H.B., BP 32 El-Alia, 16111 Bab-Ezzouar, Alger, Algeria*

<sup>c</sup> *S.C.A. – Service Central d'Analyse, U.S.R. 059 CNRS-Echangeur de Solaize, BP 22 69390 Vernaison, France*

Received 31 August 2006; received in revised form 19 January 2007; accepted 22 January 2007

Available online 8 March 2007

## Abstract

The photochemical behaviour of azoxystrobin fungicide (AZX) in water was studied under laboratory conditions. Photodegradation was initiated using a solar simulator (xenon arc lamp) or a jacketed Pyrex reaction cell equipped with a 125 W, high-pressure mercury lamp. HPLC/MS analysis (APCI and ESI in positive and negative modes) was used to identify AZX photoproducts. The calculated polychromatic quantum efficiencies ( $\phi$ ) of AZX at pH 4.5, 7 and 9 were  $5.42 \times 10^{-3}$ ,  $3.47 \times 10^{-3}$  and  $3.06 \times 10^{-3}$  (degraded molecules per absorbed photon), respectively. The relatively narrow range of values indicates the stability of AZX with respect to photodegradation in the studied pH range. Results from the HPLC/MS analysis suggest that the phototransformation of AZX proceeds via multiple, parallel reaction pathways including: (1) photo-isomerization ( $E \rightarrow Z$ ), (2) photo-hydrolysis of the methyl ester and of the nitrile group, (3) cleavage of the acrylate double bond, (4) photohydrolytic ether cleavage between the aromatic ring giving phenol, and (5) oxidative cleavage of the acrylate double bond.

© 2007 Elsevier Ltd. All rights reserved.

**Keywords:** Fungicide; Strobilurins; Azoxystrobin; Photodegradation; HPLC–MS analysis

## 1. Introduction

Strobilurin fungicides constitute a relatively new fungicide class developed from natural fungicidal derivatives such as strobilurin A, oudemansin A or myxothiazol A (Sauter et al., 1999; Bartlett et al., 2002). These compounds operate by binding at the ubiquinol-oxidation centre (Qo-site) of the bc1-enzyme complex (complex III) (Bartlett et al., 2002) of a fungi where electron transfer can take place. These well-known strobilurins have either an (*E*)-methyl methoxyiminoacetate moiety or isosteric (*E*)-methyl  $\beta$ -methoxyacrylate group which acts as a common pharmacophoric sub-structure. It has been shown that (*E*)-configured compounds exhibit a higher biological activity than

that of the corresponding (*Z*)-stereoisomers (Sauter et al., 1999).

The great impact of the strobilurin fungicides on agriculture is reflected by the widespread use of azoxystrobin (AZX), a chemical which has been approved for use on more than 80 different crops representing over 400 crop/disease systems (Bartlett et al., 2002). In recent years, much research has dealt with the behaviour of this xenobiotic in grapes, a crop of special importance in Mediterranean countries (Cabras and Angioni, 2000; Schira et al., 2002; Abreu et al., 2005; Lentza-Rizos et al., 2006). In particular, the influence of various processes on their degradation during their journey from vine to wine has been monitored in the end product (Cabras et al., 1998, 1999; Cabras and Angioni, 2000). In addition to appearing in wines, these pesticides also find their way into the environment where their behavior and ultimate fate has yet to be studied in depth. Joseph (1999) studied the abiotic degradation of AZX in three different soils. He reported that in the dark

\* Corresponding author. Tel.: +33 4 72 4327 83; fax: +33 4 72 4481 14.  
E-mail address: [jean-marc.chovelon@ircelyon.univ-lyon1.fr](mailto:jean-marc.chovelon@ircelyon.univ-lyon1.fr) (J.M. Chovelon).

and under aerobic conditions, the half-life ( $t_{1/2}$ ) of AZX was typically in the range of eight to twelve weeks and that the major metabolite formed upon degradation resulted from the hydrolysis of the ester moiety. In sterile soil there was no significant degradation. Joseph (1999) also showed that photolytic degradation is important and that a much shorter half-life of 14 d is obtained for these species under field conditions.

The aim of this work is to study the photochemical behavior of the pure, synthetic (*E*)-compounds in order to identify the largest number of photoproducts and to try to elucidate the more complete pathway for AZX photodecomposition.

## 2. Materials and methods

### 2.1. Chemicals and reagents

AZX (Methyl (*E*)-2-{2-[6-(2-cyanophenoxy)pyrimidin-4-yloxy]-phenyl}-3-methoxyacrylate) with a purity >99.6% (w/w) was used for the photodegradation experiments and were obtained from FLUKA-RIEDEL DE HAËN (SIGMA-ALDRICH CHIMIE). Standards of 2-hydroxy-benzonitrile and pirimidine-4,6-diol (purity >98% and 99% respectively) used for product identification were obtained from the same company. Acetonitrile used for HPLC analysis (HPLC grade) was purchased from Fisher Scientific and methanol for making solutions of AZX from Merck. Ultra pure water for making AZX solutions was purified with a MILLIPORE-MILLI Q system.

Working solutions were prepared by dissolving AZX in water/methanol (99:1) (v/v). Methanol was added to aid in dissolution of AZX as its solubility is only 6 mg l<sup>-1</sup> in water compared to a much larger solubility of 20 g l<sup>-1</sup> in methanol at 20 °C. Solutions were buffered by adding KH<sub>2</sub>PO<sub>4</sub> (50 mM) and adjusted to various pH values using NaOH. AZX is known to be stable with respect to hydrolysis between 25 and 50 °C and pH values ranging from 5 to 9 (Tomlin, 2000; European Commission, 1997). Nevertheless, to test for the effects of hydrolysis, experiments identical to those testing photodegradation were also carried out in the dark. All concentrations used were in accordance with the European Chemical Industry & Toxicological Centre (E.C.E.T.O.C) recommendations suggesting that, for measurements of quantum efficiency, pesticide concentrations range between 10<sup>-4</sup> and 10<sup>-5</sup> M and that solutions contain a maximum of 1% co-solvent (ECETOC, 1984; Lemaire et al., 1985).

### 2.2. Photodegradation equipment

Two borosilicate (Pyrex) reactors were used during irradiation of AZX solutions at wavelengths >290 nm. The first reactor is a solar light simulator (Suntest CPS+, HERAEUS), equipped with a 1.5 kW xenon arc lamp. The second reactor, used to accelerate the rate of photochemical degradation, was a 50 ml cylindrical vessel equipped with a

high-pressure mercury UV lamp (PHILIPS HPK 125 W). Experiments in both vessels were carried out at 19 ± 1 °C.

### 2.3. Spectrometer apparatus

The UV–visible absorption spectra were recorded using a double beam Uvikon 930 spectrophotometer (KONTRON INSTRUMENTS).

### 2.4. Kinetics experiments

Fifty millilitres aliquots of 19.8 µM AZX in water/methanol (99:1 v/v) adjusted to different pH values were irradiated for 221 h in both reactors. Samples from the solution were taken at regular time intervals for HPLC–DAD analysis without pre-concentration. The same procedure for hydrolysis experiments was carried out, but samples were kept in the dark.

### 2.5. Quantum efficiencies

Polychromatic quantum efficiency ( $\phi$ ) values were calculated using custom application software (Vulliet et al., 2002; Boudina et al., 2003). This software determines the number of absorbed photons from the pesticide absorption spectrum, the emission spectrum of the light source and the actinometric result. The kinetic measurements on the photodegradation reaction (<10% of degradation) gave the number of photodegraded molecules during the same time. Incident photonic flux was measured by chemical actinometry using uranyl oxalate purchased from Fluka. Two values were established: quantum efficiency ( $\phi_{Hg}$ ) using a high-pressure mercury lamp and quantum efficiency ( $\phi_{Xe}$ ) using a xenon lamp to forecast the AZX persistence under sunlight irradiation.

### 2.6. HPLC–DAD conditions

HPLC analyses were conducted using a SHIMADZU VP series chromatograph, equipped with a photodiode array detector (DAD). A Kromasil C<sub>18</sub> (5 µm, 150 × 4 mm) with a pore size 100 Å, and a pre-column eluted with a gradient of acetonitrile (A) and water (B) was used for the analyses. The pH during analysis was maintained at 2.8 using phosphoric acid. The following gradient was used: from 60% (B) at  $t = 0$ –25% (B) at 12 min, with this value maintained until 13 min. The flow rate was set to 1 ml min<sup>-1</sup> with an injection volume of 20 µl.

### 2.7. Solid-phase extraction

As the resulting photoproducts formed had very low concentrations, a pre-concentration step was required prior to HPLC–MS analysis. For pre-concentration, each sample was first extracted on solid-phase extraction (SPE) cartridges ISOLUTE ENV<sup>+</sup> (INTERNATIONAL SORBENT TECHNOLOGY) packed with 25 mg of highly-linked

styrene–divinylbenzene copolymer and pre-conditioned with 3 ml each of methanol then deionized water. The pre-conditioned sorbents were not allowed to dry before irradiated samples of AZX were passed through them using a Varian vacuum manifold. The pre-concentrated analytes were then eluted from the cartridges using 1 ml of methanol.

## 2.8. HPLC–MS

Photoproduct identification was performed using HPLC–MS apparatus (HEWLETT-PACKARD HP 1100 SERIES LC-MSD) equipped with a pre-column and a Kromasil C<sub>18</sub> (5  $\mu$ m, 150  $\times$  4 mm) column (column and pre-column thermostated to 25  $^{\circ}$ C). The following conditions were used: 60% (B) at  $t = 0$  to 25% (B) in 12 min, then from 25% (B) to 0% (B) in 8 min. The injection volume was 20  $\mu$ L and the flow rate set at 1 ml min<sup>−1</sup>. The MS detection was performed using ESI (electrospray ionization) and APCI (atmospheric pressure chemical ionization) in both positive and negative modes and using nitrogen as atomising gas. A capillary potential of 300 V, an N<sub>2</sub> drying gas flow of 13 l min<sup>−1</sup>, and a nebulizer pressure of 379.2 kPa (55 psi) were maintained for ESI analysis. Ionization conditions for APCI included a capillary potential of 1750 V, N<sub>2</sub> flow of 6 l min<sup>−1</sup>, and a vaporization temperature of 400  $^{\circ}$ C. Post-column addition of a mixture of CH<sub>3</sub>OH/HCOOH and CH<sub>3</sub>OH/NH<sub>4</sub>OH at a flow rate of 0.5 ml min<sup>−1</sup> using an external pump was used in order to improve the positive and negative chemical ionization respectively.

## 3. Results and discussion

### 3.1. Photophysical properties of AZX

The UV–visible absorption spectrum of AZX in aqueous solution is presented in Fig. 1. It shows a regular

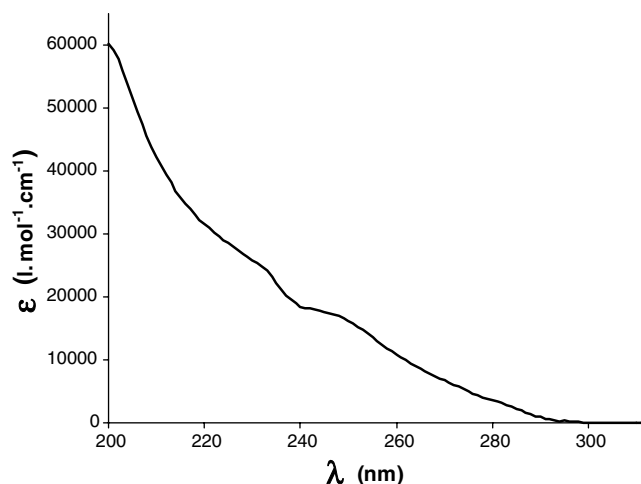


Fig. 1. Absorption spectrum of azoxystrobin in water/methanol (99:1) solution.

Table 1

Quantum efficiency ( $\phi$ ) and photochemical life-time ( $\tau$ ) of azoxystrobin taking into account Zepp's tables of sunlight irradiation in Europe and in summer

AZX in water/methanol solution (99:1) 8 ppm	$\phi$ (degraded molecules/absorbed photon)	$\tau$ (d)
High-pressure mercury lamp in a non-buffered water	$2.10 \times 10^{-3}$	16.0
High-pressure mercury lamp pH 4.5	$5.4 \times 10^{-3}$	15.6
High-pressure mercury lamp pH 7.0	$3.5 \times 10^{-3}$	18.8
High-pressure mercury lamp pH 9.0	$3.1 \times 10^{-3}$	17.0
Xenon lamp in a non-buffered water	$4.9 \times 10^{-3}$	15.0

decrease in absorbance from 200 to 300 nm with a marked shoulder at 243 nm ( $\epsilon_{243} = 18002 \text{ l mol}^{-1} \text{ cm}^{-1}$ ), a maximum at  $\lambda = 200 \text{ nm}$  ( $\epsilon_{200} = 60225 \text{ l mol}^{-1} \text{ cm}^{-1}$ ), and a characteristic band at  $\lambda = 295 \text{ nm}$  ( $\epsilon_{295} = 310 \text{ l mol}^{-1} \text{ cm}^{-1}$ ). The solar light spectrum overlaps with the absorption spectrum suggesting that direct photodegradation is possible in natural conditions. To estimate the photochemical stability of molecules, the quantum yield (for monochromatic light) or the quantum efficiency (for polychromatic light), are useful parameters to examine. In this work we have determined the quantum efficiencies of AZX in water–methanol (99:1) (Table 1) using the custom software mentioned previously. Values close to  $10^{-3}$  degraded molecules per absorbed photon were obtained for non-buffered solution using the two reactors ( $\phi_{\text{Xe}} = 4.9 \times 10^{-3}$  and  $\phi_{\text{Hg}} = 2.1 \times 10^{-3}$ ). This slight difference in values might be due to the less overlapping of the spectrum emission of solar light simulator with AZX absorption spectrum, leading to further approximation in the calculation. From this result and taking into account Zepp's tables of sunlight exposure, the software “photon” was used to calculate a value for the photolytic life-time ( $\tau$ ) of AZX under natural

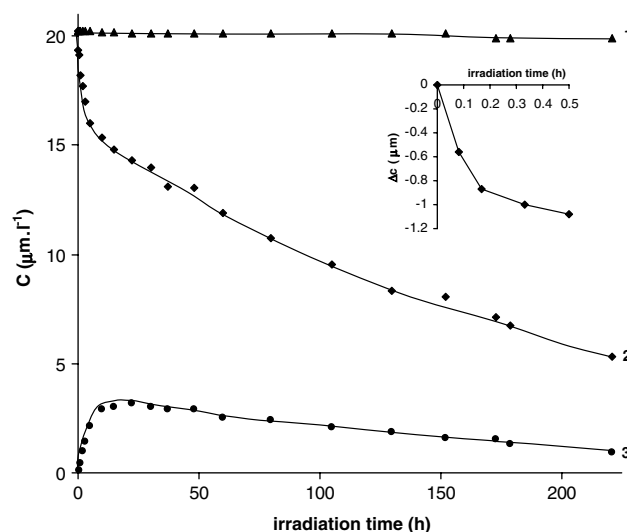
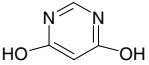
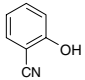
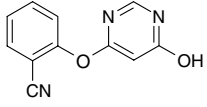
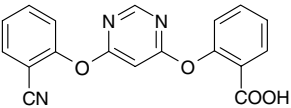
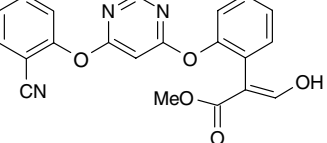
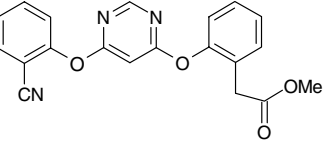
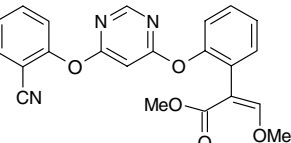
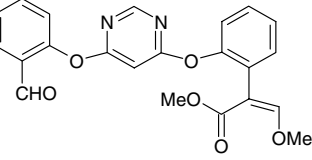


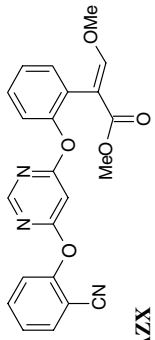
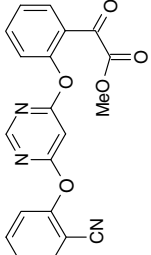
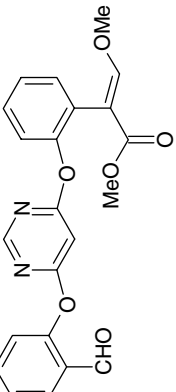
Fig. 2. (1) Evolution of AZX in dark and (2) during the irradiation using the xenon lamp (3) evolution of its Z-isomer during the irradiation using the xenon lamp (3). Inset: zoom of the variation of the concentration of AZX on the first half hour of irradiation.

Table 2  
HPLC–MS analysis of azoxystrobin after 221 h under the xenon lamp in water/methanol solution (99:1)

Compound	$R_f$ (min)	Main fragments ions ( $m/z$ ) amu ES+, ES–	Main fragments ions ( $m/z$ ) amu APCI+, APCI–	UV data (nm)
<b>A</b> 	1.1	ND	ND	$\lambda = 201; 253$
<b>B</b> 	3.0	ND	ND	$\lambda = 202; 231; 295$
<b>C</b> 	3.6	ND	214 (M+H) <sup>+</sup>	$\lambda = 193; 202; 229; 270; 280$
<b>D</b> 	6.6	334 (M+H) <sup>+</sup>	ND	$\lambda = 190; 204; 210; 256\text{--}282$ (tail)
<b>E</b> 	7.0	390 (M+H) <sup>+</sup>	ND	$\lambda = 190; 210$
<b>F</b> 	7.6	362 (M+H) <sup>+</sup> 360 (M–H) <sup>–</sup> ; 328 (M–CH <sub>3</sub> OH–H) <sup>–</sup>	362 (M+H) <sup>+</sup> 360 (M–H) <sup>–</sup> ; 328 (M–CH <sub>3</sub> OH–H) <sup>–</sup> ; 212	$\lambda = 191; 280; 216$ (shoulder)
<b>G</b> 	8.6 (Z)	404 (M+H) <sup>+</sup> ; 405; 372 (M+H–CH <sub>3</sub> OH) <sup>+</sup> more intense than in E; 373 402 (M–H) <sup>–</sup> ; 314; 212	404 (M+H) <sup>+</sup> ; 405; 372 (M+H–CH <sub>3</sub> OH) <sup>+</sup> more intense than in E; 373 402 (M–H) <sup>–</sup> ; 370 (M–H–CH <sub>3</sub> OH) <sup>–</sup> ; 435 (M–H+CH <sub>3</sub> OH) <sup>–</sup> ; 371; 356; 212	$\lambda = 226$ and 242 (shoulders); 191; 202; 280
<b>H</b> 	9.4 (Z)	407 (M+H) <sup>+</sup> ; 408; 375 (M+H–CH <sub>3</sub> OH) <sup>+</sup> 376; 317 405 (M–H) <sup>–</sup> ; 336; 316	407 (M+H) <sup>+</sup> ; 375 (M+H–CH <sub>3</sub> OH) <sup>+</sup> 405 (M–H) <sup>–</sup> ; 212	$\lambda = 191; 209; 255; 300$

(continued on next page)

Table 2 (continued)

Compound	$R_f$ (min)	Main fragments ions ( $m/z$ ) amu ES <sup>+</sup> , ES <sup>−</sup> APCI <sup>−</sup>	Main fragments ions ( $m/z$ ) amu APCI <sup>+</sup> , APCI <sup>−</sup>	UV data (nm)
 AZX	9.9 (E)	404 (M+H) <sup>+</sup> ; 405; 372 (M+H−CH <sub>3</sub> OH) <sup>+</sup> ; 373 402 (M−H) <sup>−</sup> ; 314; 212	404 (M+H) <sup>+</sup> ; 405; 372 (M+H−CH <sub>3</sub> OH) <sup>+</sup> 402 (M−H) <sup>−</sup> ; 370 (M−H−CH <sub>3</sub> OH) <sup>−</sup> ; 435 (M−H+CH <sub>3</sub> OH) <sup>−</sup> ; 371; 356; 212	$\lambda$ = 223 and 243 (shoulders); 191; 202; 280
 I	10.3	376 (M+H) <sup>+</sup> ; 318; 214	376 (M+H) <sup>+</sup> ; 214; 113	$\lambda$ = 220 (shoulder); 260–310 (tail)
 J	10.6 (E)	407 (M+H) <sup>+</sup> ; 408; 375 (M+H−CH <sub>3</sub> OH) <sup>+</sup> ; 376; 317	407 (M+H) <sup>+</sup> ; 408; 375 (M+H−CH <sub>3</sub> OH) <sup>+</sup> ; 405 (M−H) <sup>−</sup> ; 212	$\lambda$ = 191; 210; 255; 300

Retention times ( $R_f$ ), pseudo-molecular peaks (M+H)<sup>+</sup> and (M−H)<sup>−</sup> and fragments detected with electrospray ionization (positive and negative mode) and atmospheric pressure chemical ionization (positive and negative mode).  
 ND: not detected.

sunlight irradiation in Europe summer of 15 days (also see Table 1). This long lifetime implies that AZX is a relatively stable pesticide with regard to photodegradation in natural sunlight conditions.

To check whether photodegradation is pH-dependant, quantum efficiencies were measured using the high-pressure mercury lamp at three pH values. Values of  $5.4 \times 10^{-3}$  (pH 4.5),  $3.5 \times 10^{-3}$  (pH 7) and  $3.1 \times 10^{-3}$  (pH 9) were obtained demonstrating that pH does not strongly affect quantum efficiencies. This result is not surprising as AZX is not an ionic pesticide (Bending et al., 2006).

### 3.2. Kinetics studies of AZX

Fig. 2 shows the variation of AZX concentrations in (1) dark and (2) under the xenon lamp as a function of time. At natural pH values, the degradation in the dark is negligible ( $t_{1/2} = 1380$  h) while under the xenon lamp, AZX is first rapidly degraded (times less than 20–25 h) with a slower degradation thereafter. Concentration varies logarithmically with respect to irradiation time during the initial phase of photochemical transformation ( $\leq t_{1/2}$ ) (Fig. 2 inset), indicating a first order degradation process ( $\ln C/C_0$  vs time gives a straight line).

### 3.3. Identification of the photoproducts

After irradiation, pre-concentrated solutions were analysed using HPLC–MS (ESI and APCI analysis in both positive and negative modes). Table 2 shows various resulting photoproducts that have been tentatively identified and ranked according to their retention time. Compound G is assigned as the Z-azoxystrobin isomer. For this compound, the [M+H]<sup>+</sup> and [M−H]<sup>−</sup> ion products as well as the fragmentation pattern are essentially the same as for AZX, with the only difference being a 3 nm redshift in the  $\lambda_{\max}$  (UV spectra). Similar photo-induced isomerization of dienes or polyenes has been documented previously (Dugave and Demange, 2003) and so should not be surprising in AZX. Assuming identical molar extinction coefficients for Z- and E-isomers, the time-evolution of the Z-isomer concentration can be followed and is represented in Fig. 2 (curve 3). During the first 20–25 h (under the xenon lamp) the Z-isomer concentration increases and, beyond this period, decreases. By plotting the evolution of the Z/E ratio of AZX (not shown here) it has been found that during the first 20–25 h, a dramatic increase of the ratio occurs, eventually levelling off to a value around 0.25 upon reaching a photo-stationary state. It is because of this relative abundance of the Z-isomer and its similarity to the E-isomer (Joseph, 1999) that analyses was expanded to include it. Further support that this initial decrease in AZX is due mainly to photo-isomerization is that out of the original 20  $\mu$ M of AZX, 14.2  $\mu$ M of AZX and 4.6  $\mu$ M of its Z isomer are recovered after 20–25 h. Very little material was lost due to other processes during this time. Once the photo-stationary state is reached (after 20–25 h), and to

a lesser extent while photo-isomerization is occurring, both *E*- and *Z*-isomers appear to be further photolyzed at the same rate.

Photoproducts A and B (Table 2) were identified by comparison of their UV–visible chromatographic features with those of analytical standards. Photoproduct A has the same retention time and the same UV–visible spectrum ( $\lambda = 201, 253$  nm) as pyrimidine-4,6-diol. As this molecule is relatively polar, it is eluted very close to the dead volume (Fig. 3). Photoproduct B has the same retention time and UV–visible bands ( $\lambda = 202, 231$  and  $295$  nm) as 2-hydroxy-benzonitrile. It is noteworthy that 2-hydroxy-benzonitrile was also reported by Hustert et al. (2002) using GC/MS analysis in a study in which photodegradation of AZX in methanol/water (1:1) using an HPK lamp was investigated. Unfortunately, neither of these chemicals was detectable using HPLC–MS analysis. Both A and B photoproducts seem to be generated from cleavages of ether bonds of AZX.

Photoproduct (C) was identified by APCI in positive mode as being 2-(6-hydroxy-pyrimidin-4-yloxy)-benzonitrile. It should also be produced upon cleavage of one ether bond of AZX. This photoproduct was previously noted as a major photolytic product of AZX in soils (Joseph, 1999).

The minor photoproduct (E) was identified based on positive and negative mode ESI results and may be produced through demethylation of the  $\beta$ -methoxyacrylic acid moiety of AZX which involves an enolic form in equilibrium with the aldehydic one.

Photoproduct (F), presumably generated from (E) after oxidation and decarboxylation of the aldehydic form (Joseph, 1999) was tentatively identified as {2-[6-(2-cyano-phenoxy)-pyrimidin-4-yloxy]-phenyl}-acetic acid methyl ester. Only one peak ( $R_t = 7.6$  min) (Fig. 3) was observed

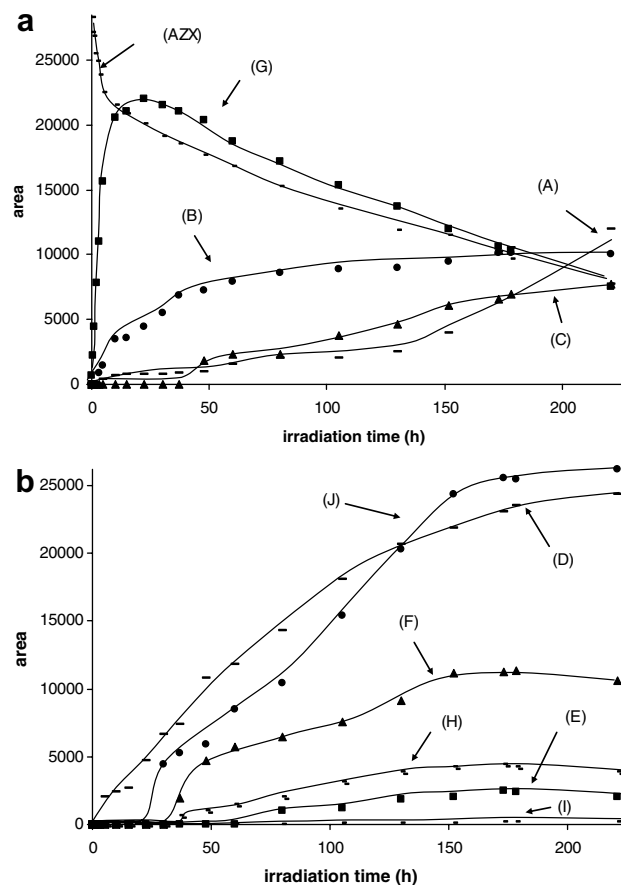


Fig. 4. (a) Evolution of the principal photoproducts obtained during xenon lamp irradiation of AZX. In these figures, (AZX) and (G) areas were divided by 33 and 10, respectively. Area determination at  $\lambda = 220$  nm. (b) Evolution of photoproducts D, F, J, H, E and I as a function of the xenon lamp irradiation time. Area determination at  $\lambda = 220$  nm.

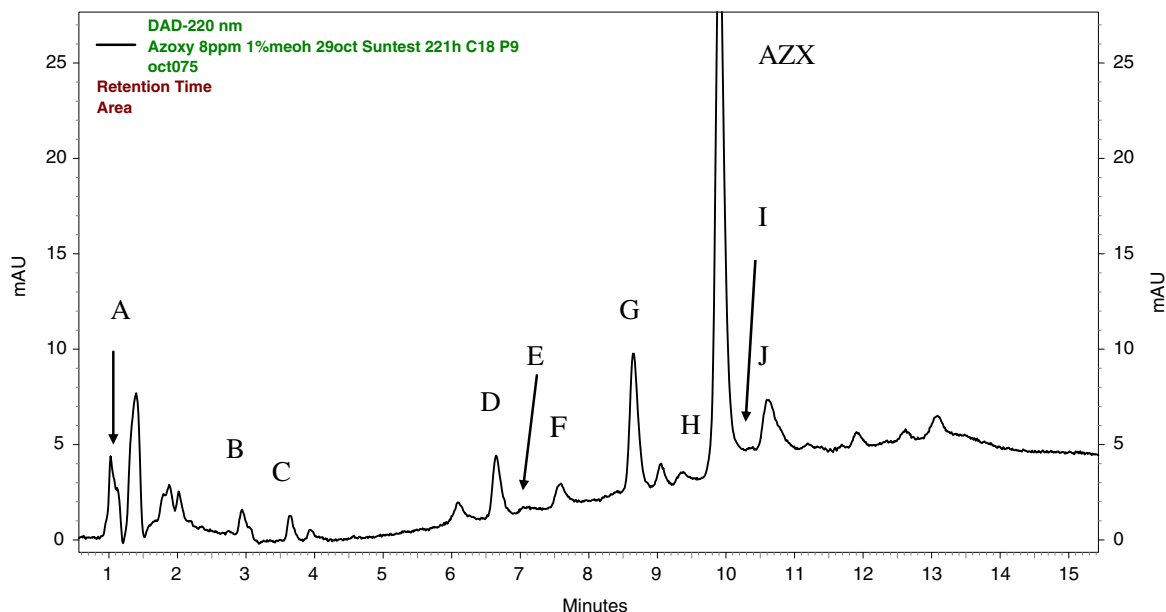


Fig. 3. HPLC chromatograms of azoxystrobin after 221 h of xenon lamp irradiation. Detection at  $\lambda = 220$  nm.

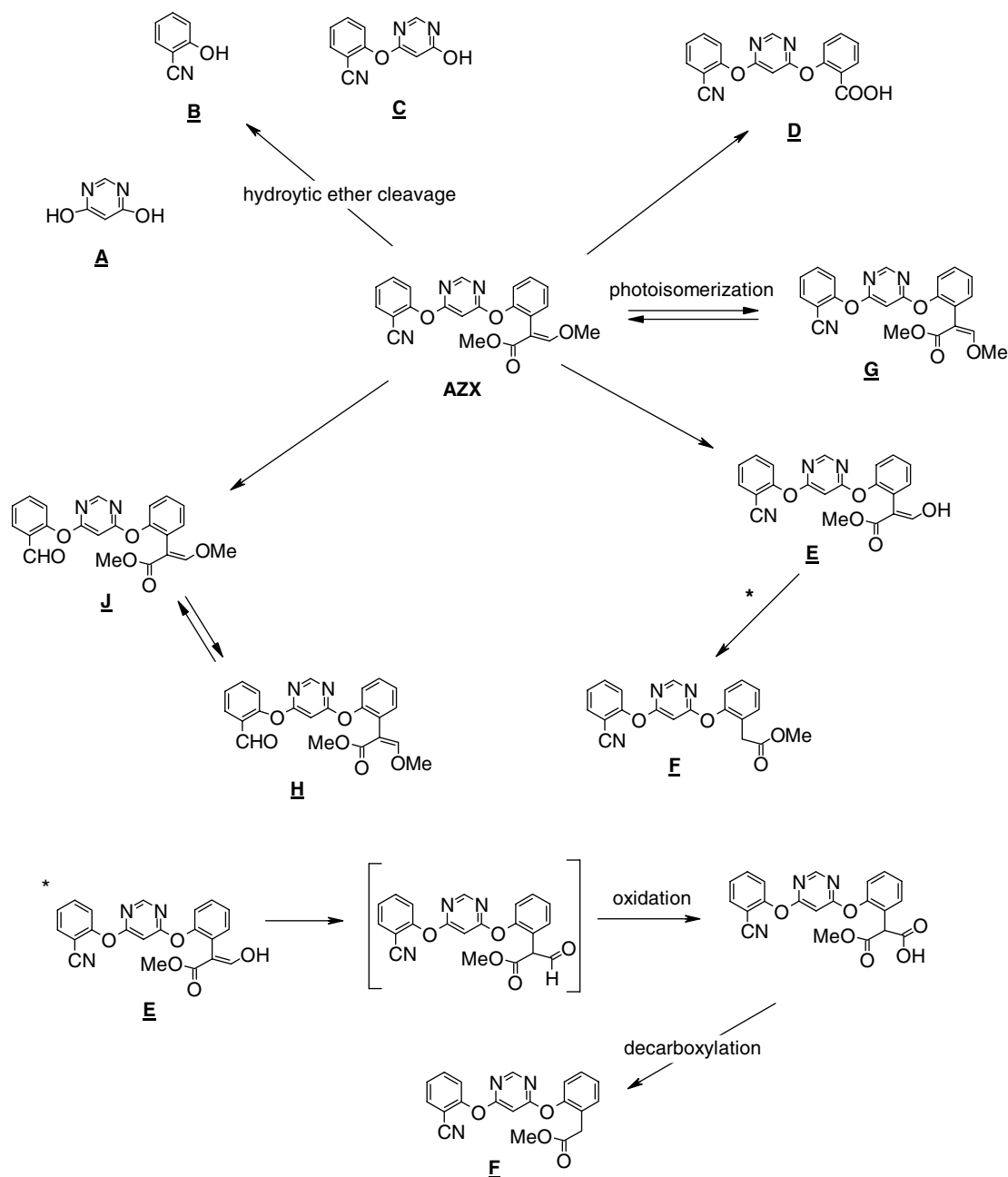


with its characteristic mass spectrum suggesting that F does not have any isomeric forms.

Oxidative cleavage of the acrylate double bond, yields compound I in very low amounts. Compound I was identified by positive mode ESI and APCI as {2-[6-(2-cyano-phenoxy)-pyrimidin-4-yloxy]-phenyl}-oxo-acetic acid methyl ester. This product was in turn oxidized to give photo-product D which was identified by positive mode ESI as 2-[6-(2-cyano-phenoxy)-pyrimidin-4-yloxy]-benzoic acid. Compound (D) was also reported as a main photolytic product in earlier field dissipation studies of AZX (Joseph, 1999). Only a single eluted peak was observed for both

compounds I and D, once again suggesting only a single isomeric form for each of these species.

To our knowledge, photoproducts H and J have not been observed before in studies of AZX. We have identified these new products as two isomers of 2-{2-[6-(2-formyl-phenoxy)-pyrimidin-4-yloxy]-phenyl}-3-methoxy-acrylic acid methyl ester. As the molecular weight of these compounds are even numbers (406 uma), the molecular weight parity rule indicates that both have an even number of nitrogen atoms. Photo-hydrolysis of the nitrile-group to give the corresponding aldehyde form is a potential path that might lead to their production. Bonnichon and



Scheme 1. Tentative pathway for photochemical degradation of azoxystrobin in an aqueous solution. \* Proposition for the formation of photoproduct F.

Richard (1998) have reported a similar reaction concerning the photodegradation of 3-hydroxy-benzonitrile in water since 3-hydroxybenzaldehyde was obtained at all pHs tested. In our case, the photoproducts seem to retain the (*E/Z*) isomerism of their precursor, with the *E*-isomer (Compound J) obtained in higher yield than the *Z*-isomer (Compound H).

#### 3.4. Kinetics of the main photoproducts

Fig. 4a shows kinetic curves for AZX, A, B, C, and G obtained after irradiation of AZX using the xenon lamp and followed by HPLC–DAD. Almost 72.7% of AZX is degraded to some other form after 221 h of irradiation with compound G being the most prominent chromatographic peak area. Both photoproducts B and A seems to appear at low concentration immediately upon irradiation and accumulate in the solution without any further degradation. Using chemical standards, 1.29  $\mu\text{M}$  concentrations of photoproduct B were confirmed after 221 h of irradiation, a level maintained for all times after 20–25 h. The product C appears in the last position meaning that surely it comes from other photoproducts.

Fig. 4b shows the evolution of photoproducts E, F, H, I, and J which appear following the photo-isomerization reaction 20–25 h after the start of irradiation. We hypothesize that AZX gives rise to E which in turn is transformed into F. These photoproducts also seem to be quite stable from the photochemical point of view.

Based on the presented structural information and the kinetics of their degradation and appearance, a possible pathway for the photolytic degradation of AZX in water is proposed in Scheme 1.

#### 4. Conclusion

AZX in aqueous solution absorbs light at wavelengths higher than 290 nm and can therefore be photodegraded in the environment. Ten photoproducts have been tentatively identified as coming either from photo-isomerization or photolytic degradation of this pesticide.

Photo-isomerization of AZX is a very fast reaction, occurring immediately upon irradiation. A photo-stationary state between *Z*- and *E*-isomers was obtained after 20–25 h. Other photoproducts were mainly generated after reaching the photo-stationary state. In addition, it has been shown that some photoproducts were intermediates subject to further degradation while others might accumulate in the environment.

#### Abbreviations

AZX	azoxystrobin
$\epsilon_\lambda$	molar extinction coefficient
$t_{1/2}$	time of half reaction ( $\ln 2/k$ )
$\tau$	photolytic life-time
$\phi$	quantum efficiency
$R_t$	Retention times

ESI	electrospray ionization
APCI	atmospheric pressure chemical ionization
( $M+H$ ) <sup>+</sup>	molecular peak detected with ESI or APCI in positive mode
( $M-H$ ) <sup>−</sup>	molecular peak detected with ESI or APCI in negative mode
E.C.E.T.O.C	European Chemical Industry & Toxicological Centre

#### Acknowledgements

The authors are grateful to Robert BAUDOT (S.C.A.) for HPLC/MS analyses and for helpful suggestions in the spectra interpretations. We thank Dr. Thomas CUSTER from Max-Planck-Institute for Chemistry in Mainz, Germany for improving the English of the manuscript. Finally, The Editor and Reviewers are thanked for their effort and contribution to the improvement of the paper content.

#### References

- Abreu, S. de Melo, Correia, M., Herbert, P., Santos, L., Alves, A., 2005. Screening of grapes and wine for azoxystrobin, kresoxim-methyl and trifloxystrobin fungicides by HPLC with diode array detection. *Food Addit. Contam.* 22 (6), 549–556.
- Bartlett, D.W., Clough, J.M., Godwin, J.R., Hall, A.A., Hamer, M., Parr-Dobrzanski, B., 2002. Review: the strobilurin fungicides. *Pest Manage. Sci.* 58, 649–662.
- Bending, G.D., Lincoln, S.D., Edmondson, R.N., 2006. Spatial variation in the degradation rate of the pesticides isoproturon, azoxystrobin and diflufenican in soil and its relationship with chemical and microbial properties. *Environ. Pollut.* 139, 279–287.
- Bonnichon, F., Richard, C., 1998. Phototransformation of 3-hydroxy-benzonitrile in water. *J. Photochem. Photobiol. A* 119, 25–32.
- Boudina, A., Emmelin, C., Baaliouamer, A., Grenier-Loustalot, M.F., Chovelon, J.M., 2003. Photochemical behaviour of carbendazim in aqueous solution. *Chemosphere* 50, 649–655.
- Cabras, P., Angioni, A., 2000. Reviews: pesticides residues in grapes, wine, and their processing products. *J. Agric. Food Chem.* 48 (4), 967–973.
- Cabras, P., Angioni, A., Garau, V.L., Pirisi, F.M., Espinoza, J., Mendoza, A., Gabitza, F., Pala, M., Brandolini, V., 1998. Fate of azoxystrobin, fluazinam, kresoxim-methyl, mepanipyrim, and tetraconazole from vine to wine. *J. Agric. Food Chem.* 46, 3249–3251.
- Cabras, P., Angioni, A., Garau, V.L., Pirisi, F.M., Farris, G.A., Madau, G., Emonti, G., 1999. Pesticides in fermentative processes of wine. *J. Agric. Food Chem.* 47, 3854–3857.
- Dugave, C., Demange, L., 2003. Cis–trans isomerization of organic molecules and biomolecules: Implications and applications. *Chem. Rev.* 103, 2475–2532.
- E.C.E.T.O.C., Technical Report No. 12, 1984. Determination of phototransformation of chemicals in water: results of a ring test. Brussels, Belgium.
- European Commission, 1997. Azoxystrobin. Monograph prepared in the context of the Council Directive 91/414/EEC, European Commission, Brussels, Belgium, Rev. 5, vol. 4, annex 1.
- Hustert, K., Feicht, E.A., Kettrup, A., 2002. Photodegradation of azoxystrobin and kresoxim-methyl under simulated environmental conditions. *Fresen. Environ. Bull.* 11 (7), 322–325.
- Joseph, R.S.I., 1999. Metabolism of azoxystrobin in plants and animals. In: Brooks, G.T., Roberts, T.R. (Eds.), *Pesticide Chemistry and Bioscience, The Food Environment Challenge*. The Royal Society of Chemistry, Cambridge, UK, pp. 265–278.



- Lemaire, J., Guth, J.A., Klais, O., Leahey, J., Merz, W., Philp, J., Wilmes, R., Wolff, C.J.M., 1985. Ring test of a method for assessing the phototransformation of chemicals in water. *Chemosphere* 14 (1), 53–77.
- Lentza-Rizos, C., Avramides, E.J., Kokkinaki, K., 2006. Residues of azoxystrobin from grapes to raisins. *J. Agric. Food Chem.* 54, 138–141.
- Sauter, H., Steglich, W., Anke, T., 1999. Strobilurins: evolution of a new class of active substances. *Angew. Chem., Int. Ed.* 111, 1416–1438.
- Schira, M., Cabras, P., Angioni, A., Brandolini, V., 2002. Residue levels and storage decay control in Cv. Star ruby grapefruit after dip treatments with azoxystrobin. *J. Agric. Food Chem.* 50, 1461–1464.
- Tomlin, C., 2000. *The Pesticide Manual: A World Compendium* Farnham, Surrey, 12th ed. British Crop Protection Council, UK, pp. 70–71.
- Vulliet, C., Emmelin, C., Grenier-Loustalot, M.F., Paissé, O., Chovelon, J.M., 2002. Simulated sunlight-induced photodegradation of triasulfuron and cinosulfuron in aqueous solution. *J. Agric. Food Chem.* 50, 1081–1088.